



Automatic detection for Extreme-ultraviolet solar coronal bright points

Hossein Safari, Azar Nasiri and Nasibe Alipour

Here, we aim to automatic detection of extreme-ultra violet solar coronal bright points observed by Atmospheric Imaging Assembly (AIA). The method is based on machine learning SVM classifier and image Zernike moments. The size frequency distributions of detected bright points show the lognormal behaviors. Around 3 percent of solar surface is covered by solar coronal bright points.

PACS numbers: 05.10.-a ,05.10.Gg, 98.70.Vc

I. INTRODUCTION

This Coronal bright points (solar coronal bright points) were observed on the X-ray and extreme-ultraviolet images [1]. Coronal bright points with the size less than 60 arcsec are appeared on the solar atmosphere and their lifetimes are ranged from a few minutes to few days [2]. A majority of solar coronal bright points are associated with canceling magnetic bipoles and a small percentage of them are related to the ephemeral active region [3]. SDO/AIA is providing full Sun images through UV and EUV filters. Here, using an automatic detection algorithm by using SVM and invariants of Zernike moments, the solar coronal bright points are recognized.

II. METHOD

Coronal bright points detection methods are developed based on intensity characteristics as compared with background [4, 5]. The following steps are employed to recognised bright points from 193 Å AIA images:

- Coronal bright points are mostly seen in quiet sun regions and coronal holes. In active regions they disappear into the general background activity there is too much line-of-sight confusion. We selected coronal bright points for training classifier network. According to Sattarov et al., (2010), we select potentially bright points that are centered to an image-tile with radius greater than 2 Mm (3 arcsec) and less than 20 Mm (28 arcsec). Their shapes would not elongated and crescent-like structures In Figure 1, a typical light-curve of a CBP in three phases is shown. The final selected bright points (700 bright points) are used as class 1 of our training data set. In class 2, some non-bright points features with sample spatial sizes (60"×60") are selected. In Figure 2, samples of selected CBPs and non-CBPs are shown.
- The Zernike moments of each image tiles of bright points and non-bright points image-tiles are com-

puted. The magnitudes of the moments are fed to the SVM classifier. Now, the network classifier are ready to use.

- For each images of size 4096×4096 from 193 Å data set, were calibrated and de-rotated, imagetile, starting from $x_1 = 1$ and $y_1=1$ with the size $\Delta x=20$ and $\Delta y=20$ is extracted.

The Zernike moments of this image-tile is computed and the magnitudes of the moments are fed to the SVM classifier. The code picks up a label 1 for a bright point feature and 2 for a non-bright point feature. If it is a bright point, the locations (x_{max} , y_{max}) and time t are saved. Then the small box is moved first in x-direction until the end of the grid is reached and then in y-direction.

III. RESULTS AND DISCUSSION

Using the automatic detection method, the coronal bright points of full disk 193 Å SDO/AIA images are recognized. The recognized bright points with distances of their brightness centers (the position of maximum value of brightness) larger than 60 arcsec are called "separate events". For distances smaller than 60 arcsec, using the Region Growing (RG) algorithm the pixels (R_i) of each bright points are determined. Also, two bright points with separate pixels, $R_i \cap R_j = \emptyset$, we know as "separate events". On 20 hours period of study of AIA images, the average numbers of 600 coronal bright points (separate events) per image are detected. These average numbers are twice of Sattarov et al. (2010) and Zhang et al. (2001). In Figure 3, samples of identified CBPs (marked with red contours) are presented. As we see, the considerable number of faint and small bright points are detected. Javaherian et al. (2014), have shown that the structures of Zernike moments are distinctive enough to identify the faint and bright features with various sizes and different rotation angles using a SVM classifier [6]. The disagreement between the number of bright points





with previous studies (e.g., Sattarov et al., 2010) may be depend on spatial resolution of data as used and performances of recognition algorithms.

The frequency distribution of size of bright points as a function of the sizes (A) in log-log scale is shown in Figure 4.

$$f = \frac{\sum_{i=1}^N A_{BC}^i}{A_{Sun}}$$

The filling factor of bright points for a full disk image is given where, N is the number of observed CBPs and A_{Sun} is the area of solar surface within ± 60 longitude and latitude. The evolution of the filling factor of bright point cores, and their distributions are shown in Figures 5. The filling factor is ranged in 0.012-0.017. This gives 3 percentage of solar surface is covered by area of bright points and twice of Zhang et al. (2001).

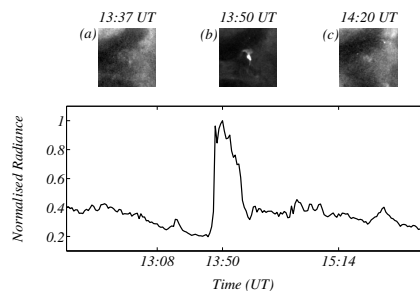


FIG. 1. Temporal evolution of a CBP. A typical light cure of the coronal bright point.

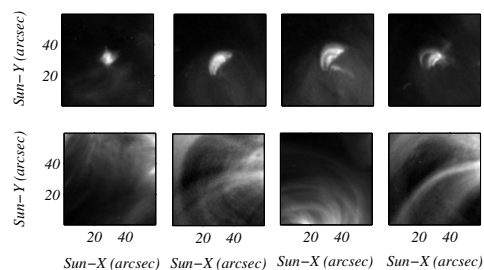


FIG. 2. Various samples of CBPs and non-CBPs are presented.

[1] Golub, L., Krieger A. S. *et al.*, 1974, ApJ, 189, L93.
 [2] Zhang, J., Kundu M. R. *et al.*, 2001, Sol. Phys, 198, 347.
 [3] Priest, E. R., Parnell, C. E. *et al.*, 1994, ApJ, 427, 459.
 [4] McIntosh, S. W., & Gurman J. B. 2005, Sol. Phys, 228, 285.
 [5] Sattarov, I., Pevtsov, A. *et al.*, 2010, Sol. Phys, 262, 321.
 [6] Javaherian, M., Safari, H., Amiri, A., & Ziaei, S. 2014, Sol. Phys., 289, 3969.

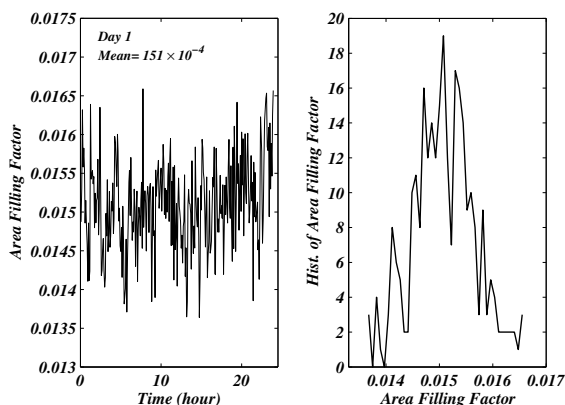


FIG. 5. The evolution of the filling factor of CBPs, and their distributions for 7 June 2010 are shown.

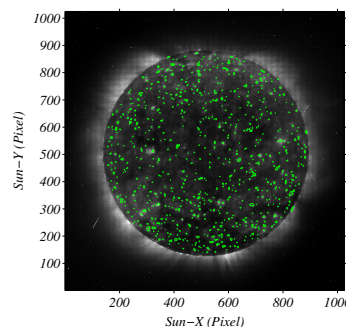


FIG. 3. SoHO/EIT full disk image at 195 Å on 16 February 2008 00:00 UT. The locations of CBPs (green contours) recognized by presented algorithm are shown.

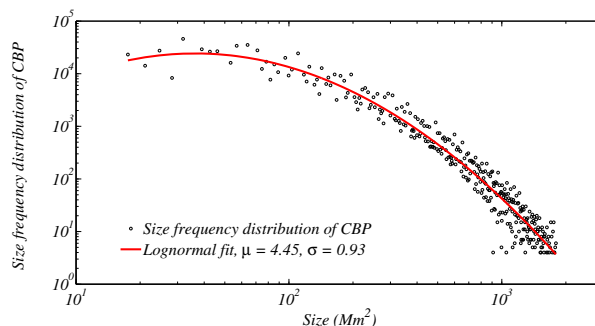


FIG. 4. The frequency distribution of size of CBPs versus size in log-log scale are shown.

